SSRG International Journal of Electronics and Communication Engineering
ISSN: 2348-8549/ https://doi.org/10.14445/23488549/IJECE-V10I7P102

Volume 10 Issue 7, 13-22, July 2023

Original Article

GLCM Features and Fuzzy C Means Clustering-Based Brain Tumor Detection in MR Images

S. Bhuvaneswari[1], R. Surendiran[2], S. Satheesh[3], Kavitha V Kakade[4], M. Thangamani[5], P. Thangaraj[6]

[1]*Department of BCA, Annai College of Arts and Science, Kumbakonam, Tamilnadu.*
[2]*School of Information Science, Annai College of Arts and Science, Tamilnadu.*
[3]*Department of Computer Science and Engineering, Arjun College of Technology, Tamilnadu.*
[4]*Anna University, Tamilnadu, Chennai.*
[5]*Department of Computer Science and Engineering, Hindusthan Institute of Technology, Coimbatore, Tamilnadu.*
[6]*Department of Computer Science and Engineering, Builders Engineering College, Kangeyam, Tamilnadu.*

[2]*Corresponding Author : surendiranmca@gmail.com*

Received: 18 April 2023 Revised: 19 June 2023 Accepted: 10 July 2023 Published: 31 July 2023

Abstract - *Identifying and categorizing human brain tumors are labour-intensive activities, yet they are crucial for any doctor. There is a growing trend toward using computer-assisted diagnosis (CAD) to improve diagnostic abilities and raise detection accuracy to the highest possible levels. Variability in picture modality, contrast, tumor kind, and other characteristics makes brain tumor segmentation a difficult problem to solve despite years of study. Though there are many excellent works accessible, there is still a need for the development of efficient and precise ways for tumor segmentation with MR brain images. To address this gap in the literature, researchers have developed a new method for detecting human brain cancers that combines a template-based K-means (TK) algorithm, superpixels, and principal component analysis (PCA) to achieve faster detection rates while requiring less processing time overall. Super pixels and PCA can be utilized to identify the most useful information for the early detection of brain cancers. Then, a filter is used on the enhanced image to boost precision. Finally, the TK-means grouping technique is considered for subdividing the pictures for brain tumor identification. Super pixel-based feature extraction, on the other hand, leads to subpar segmentation results since it relies on region-based feature calculation rather than attempting to extract every possible feature from the brain pictures. Once the images have been improved by converting colour into grayscale, the Gray Level Co-Occurrence Matrix (GLCM) approach is utilized to extract the five statistical texture parameter features. Reduce the file size of an image by using a dimensionality reduction technique like the Independent Component Analysis (ICA) model. Finally, brain tumors are identified, and their segmentation is performed with the help of Fuzzy C Means clustering (FCM). The results obtained from a broad set of images further demonstrate the usefulness of the suggested model for recognizing the sizes and shapes of brain tumors.*

Keywords - *Tumor detection, Segmentation, Image enhancement, Dimensionality reduction, Fuzzy C Means clustering.*

1. Introduction

The brain tumors known as gliomas can metastasize to neighbouring brain areas. Without prompt diagnosis and treatment, gliomas can be fatal. The WHO reports that adult mortality rates are greater than child mortality rates. Cancer.net reports that this year there will be 23,820 new cases of adult brain tumors and 5270 new cases of paediatric brain tumors in the United States. Age, tumor type, and tumor site all play a role in how a brain tumor is treated [1-3]. Diagnosing and treating cancers that have spread to neighbouring healthy tissue might be challenging. Therefore, early detection of brain tumors by accurately segmenting them from surrounding tissues is crucial for increasing patients' chances of survival. Images of brain tumors are typically captured using magnetic resonance imaging (MRI). The MRI scanner's settings allow for the acquisition of various modalities [4, 5].

Due to their complex structure and appearance, the tumor borders are frequently fuzzy, and tumors may move into the nearby area of the brain; making MRI images, it is challenging to tell the diseased tissue apart from the surrounding healthy tissue, making accurate tumor segmentation a challenging task. Because of this, manually delineating tumor boundaries in MRI scans is laborious and sometimes inaccurate. The nature and location may be determined by automatically segmenting brain tumors from MRI scans, allowing for a rapid and accurate diagnosis. Patients may be cured if cancers are detected and treated early enough through the K-NN algorithm[6].

The existing study proposed an improved brain tumor detection strategy for automated brain tumor segmentation based on the TK algorithm with superpixels and PCA, effectively identifying human brain malignancies to develop faster than expected. Super pixels and PCA can be utilized to identify the most helpful information for the early detection of brain cancers. Then, a filter is used on the enhanced image to boost precision. Finally, the TK-means clustering approach helps segment the images for tumor detection in the brain. Super pixel-based feature extraction, on the other hand, leads to subpar segmentation results since it relies on region-based feature calculation rather than attempting to extract every possible feature from the brain pictures when trying to cluster data. K-means struggle when clusters vary in size and density.The input brain MRI data is improved through pre-processing in this work by converting colour images (RGB) to a grayscale image and eliminating noise with a median filter. Once the images have been improved, GLCM, the five statistical texture parameters' characteristics are extracted using a technique. Reduce the file size of an image by using a dimensionality reduction technique like the Independent Component Analysis (ICA) model. Finally, brain tumors are identified, and their segmentation is done with Fuzzy C Means clustering (FCM)[7, 8].

2. Literature Review

Manogaran et al. [9] examined the areas of brain tumors under and over-segmented using an Improved Orthogonal Gamma Distribution-based Machine-Learning Approach (IOGDML) for automatic ROI abnormality detection. By sampling the sensitivity in the aberrant area and edge coordinates, the machine learning system can assess the selectivity parameters and correct any further data imbalances caused by poor edge matching[10]. It created and investigated the benchmark medical image datasets to verify the efficacy and precision of the best-automated detection in tumor and non-tumor zones. The algorithm's mean error rate was calculated using a mathematical model. Experiments used to test the system found that the orthogonal gamma distribution method combined with a machine learning methodology successfully detected brain tumors with a success rate of 99.55 percent. This study aids in developing automated methods for analyzing brain abnormalities in the medical area[11].

Vijay and Subhashini [12] discussed an effective approach to automatic brain tumor segmentation for isolating tumor tissues in MR scans. The K-means clustering technique is taken to do the segmentation in this approach. Compared to many other clustering techniques, this one is lightning fast while significantly improving the tumor borders. The outcomes achieved by using the offered method are highly regarded. Amsaveni and Singh [13] demonstrated a computational strategy for delineating the brain tumor location in MRI scans. Pre-processing, feature extraction, and classification through neural network methods are all built into the algorithm. Gabor filter enabled the extraction of textural features in the identified tumor. The features are fed into an Artificial Neural Network classifier that is then utilized for training and labelling diagnoses of brain tumors[14]. The technique vastly enhances the classifier's precision when looking for brain tumors. Rina Mahakud [15] applied an MRI image for tumor detection inside the kidney. Chaddad et al. [16] are concerned with a novel Glioblastoma (GEM) detection features type that depends on the Gaussian Mixture Model (GMM). We discuss using Tl, T2, and FLAIR MR images in conjunction with the novel feature to locate the tumor in the brain. The performance achieved with the feature-based approach for detecting brain tumors is enhanced through the use of multi-thresholding segmentation carried out with morphological operations of MR images, and the redundant and confusing regions are removed.

Using assess the value of cancer and usual area diversity on the GMM features, a decision tree classifier is used whose reduction is done with three main components. Including the photographs, the distinction between GEM and the regular region was performed regarding false alarm, precision and missed detection measures; MRI imaging modes—Tl, T2, and Flair—were also used. The GMM features showed good performance. There was no missed detection or false alarm rate of 0% for either the Tl or T2 weighted pictures. If you switch to FLAIR mode, your precision drops to 94.11%, with a corresponding increase in false alarms and misses detections of 2.95 percent.

All of the trial outcomes are encouraging for advancing early GEM diagnosis. Identification of the Brain tumor using MRI, CT-scan images carried out by [17-21]. The different brain mass lesions with histopathological correlation can be found by [22]. To find the role of specious diffusion coefficient values in the classification and diversity of benign and malevolent mass injuries of the brain. The brain tumor detection system helps doctors [23] decide on patient treatment for removing tumor growth. Different types of classification methods are applied. This author used multi-class SVM and deep learning techniques of AlexNet. This handles imbalanced data and gives expected accuracy[24]. The authors [25] focused the signal noise suppression using independent component analysis.

3. Proposed Methodology

This subsection elaborates on the proposed model for detecting brain tumors. First, a median filter is utilized to remove the noise once the picture is converted from colour to grayscale; the second stage includes feature extraction by applying a GLCM; the third stage consists of dimensionality reduction with Independent Component Analysis, and the fourth step is to use Fuzzy C Means clustering (FCM) to locate and segment brain tumors. Figure 1: Overarching design of the planned work.

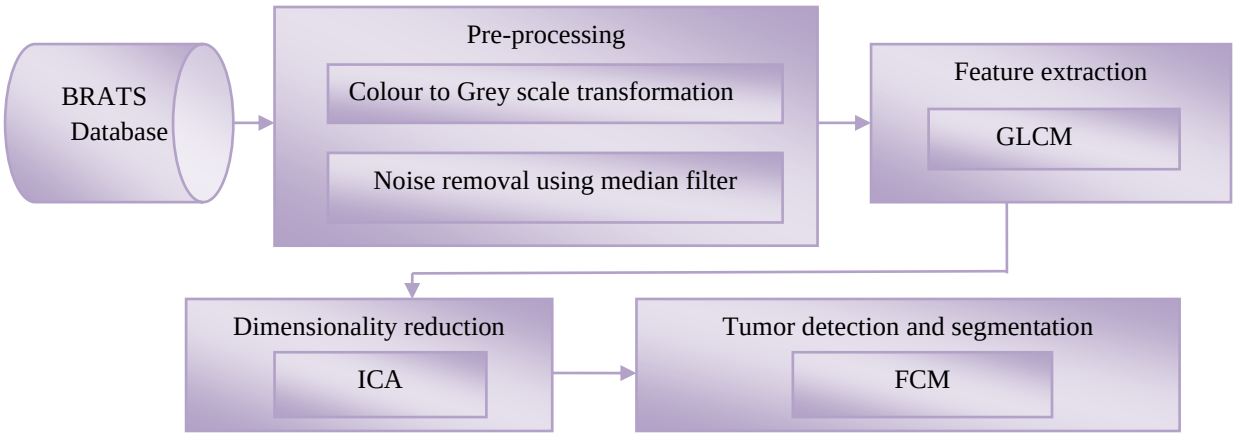

Fig. 1 Architecture-proposed brain tumor detection

3.1. Input Data

The suggested brain tumor detection model uses the publicly available kaggle dataset consisting of 310 brain images, of which 200 are yes-class and 100 are no-class samples.

70%, 30% of the information is utilized for assessment, and the remaining 40% is for learning. The outcome is verified by using both the training and testing datasets.

3.2. Pre-Processing

The pre-processing stage intentions to progress the product's value images to be used in the subsequent detection phase. Next, a filter is used to suppress any residual noise from the image after it has been converted from its original colour space (RGB) to grayscale.

3.2.1. Noise Removal using Median Filtering

Median filtering, the most common nonlinear filtering approach, effectively weakens the interference pulse while preserving the signals' original properties.

This is why it is commonly employed as a pre-processing method [25]. When the signal length is N, the filtering window length is described as n. The filter's output can be expressed as

$$med(a_i) = \begin{Bmatrix} a_{k+1} n = 2k+1 (odd) \\ \frac{[a_k + a_{k+1}]}{2} \; n = 2k (even) \end{Bmatrix} \quad (1)$$

Here a_k refers to the k-th maximum observed data, and a_1, a_2, a_3...a_k are the observed data. The median filter's standout feature is how it can remove pulse noise while preserving localized information.

Following this process, the final image is sent to the feature extraction block, where the GLCM is used to draw out specific characteristics from the images.

3.3. Feature Extraction using Gray Level Co-occurrence Matrix (GLCM)

When estimating picture features connected to second-order statistics [26, 27], the GLCM is a useful tool. Here are how the texture features are calculated:

Energy: Energy is a measure of how consistent the mammogram seems. The mean squared signal value is typically used to estimate the energy level. The formula for calculating it is as given.

$$\text{Energy} = \sum_{i,j=0}^{n-1} p(i,j)2 \quad (2)$$

The contrast is the difference between the minimum and maximum values in a set of nearby pixels. It computes how many small changes there are in the image.

$$\text{Contrast} = \sum_{i,j=0}^{n-1} (i-j)^2 p(i,j) \quad (3)$$

The correlation between a pixel and its neighbour is quantified here.

$$\text{Correlation} = \sum_{i,j=0}^{n-I} \frac{(i \times j) p(i,j) - u_i u_j}{\sigma_i \sigma_j} \quad (4)$$

σ2 = the difference found in the intensities of all the reference pixels in the correlations, contributing towards the GLCM, calculated as below:

$$\theta^2 = \sum_{i,j=0}^{N-1} p_{i,,j} (i-u) \quad (5)$$

Homogeneity, Angular Second Moment (ASM): ASM is utilized in order to gauge the amount of homogeneity in the image

$$\text{Homogeneit} \sum_{i=0}^{n-1} \sum_{j=0}^{n-1} \{p(i,j)\}^2 \quad (6)$$

Entropy: Entropy measures the unevenness or complexity present in the image. Entropy yields the maximum value when the assignment of P (i, j) is uniform throughout the matrix. Entropy has a large but inverse correlation with energy.

$$\text{Entropy} = -\sum_{i,j=0}^{n-1} p(i,j)\log p(i,j) \quad (7)$$

Where 'i' specifies the rows of the GLCM matrix, 'j' refers to the columns of the GLCM matrix, 'n' indicates the number of gray levels, and P(i, j) refers to the cell that the row and the column of the GLCM matrix represent. Based on these evaluations, the texture features are extracted.

3.4. Dimensionality Reduction using ICA

This work applies ICA to make the features' dimensions smaller, which were retrieved. The central concept behind ICA is to assume that a number of statistically independent sources linearly mix data and then demix these signal sources based on their mutual information. In order to ensure the validity of the method, it assumes that no more than one of the sources in the ensemble model is a Gaussian source [28, 29].

$$X=AS \quad (8)$$

Where A stands for an $L \times p$ a p-dimensional signal source vector denoted by collaborative matrix and s calls for separating p signal sources. The goal of the ICA is to get a demixing matrix (demixing matrix w), which aids in dividing the source vectors s into a number of statistically independent sources. Various other conditions have been introduced for measuring source independence. However, they all grew out of the idea of mutual information, a metric for gauging the difference between two independent random sources [30].

Assume that x and y are zero mean p-dimensional support random source vectors [31] with covariance matrices. This is a superior case of the previous equation of (8).

$$\sum_x = \left(\frac{1}{p}\right)[XX^T] \quad (9)$$

and

$$\sum_y = \left(\frac{1}{p}\right)[YY^T] \quad (10)$$

Correspondingly, For decorrelating x in the same manner that x is the demixed in (8), a whitening matrix $\sum_x^{-1/2}$ matrix whose covariance is determined by the inverse of the square root of its own variance $\sum_x$ can be utilized for whitening the signal source vector x. Consequently,

$$\sum_y = \left(\sum_x^{-\frac{1}{2}}\right)\sum_x\left(\sum_x^{-\frac{1}{2}}\right)^T = I \quad (11)$$

Moreover, the resultant source vector y goes on to be an uncorrelated signal source vector (Egan vector) analogous to signal source vector s in equation (1) to produce a statistically independent source vector via the use of a demixing matrix w obtained by the ICA through the use of (8). In place of this definition, the number (8) is shortened to

$$x=\sum_x^{1/2} y \implies y = \sum_x^{-1/2} x \quad (12)$$

The square root of the covariance matrix helps to replace the collaborative matrix A and the source vector in (8) $\sum_x^{1/2}$, and a random source vector y with no correlation, correspondingly.

As per (12), PCA reduces the second-order statistics decorrelation's statistical independence as assessed by the ICA. In line with this, the ICA actually does the PCA using a whitening matrix on the p-dimensional associated signal basis vector x $\sum_x^{-1/2}$ to produce p-not-associated PCs that, in terms of second-order statistics, reflect the uncorrelated signal source vector [36]. In signal processing and communications, decorating a source vector of second-order statistics called x into a not associated source path of signal called y consuming equation (12) is often referred to as whitening. $\sum_x^{-1/2}$ is being utilized in the form of a whitened matrix. The sole dissimilarity between (8) and (12) is that the mixing matrix A in (8) is not known, contrary to the covariance matrix. $\sum_x^{1/2}$ (12), this is easily calculable using just the observed signal source vector x.

3.5. Brain Tumor Detection and Segmentation using Clustering FCM

After dimension reduction, detection and segmentation are conducted in this study utilizing clustering FCM. The FCM algorithm is prevalent in image segmentation among the fuzzy clustering techniques since it contains the best qualities to deal with anomalies. While soft segmentation techniques like spatial FCM can keep much data, hard segmentation approaches cannot. In FCM, pixels are distributed among classes using fuzzy membership functions.

The algorithm determines whether or not a given data point belongs to a given cluster based on its distance from the cluster's center. The nearer some data is to the centre of a cluster, the more probably it is to belong to that cluster. One can easily see that the total number of members should equal one if all the data points are added together [32, 33]. Following every iteration, the membership and cluster centres are revised using the following expression:

$$\mu_{ij} = 1/\sum_{k=1}^{c}\left(d_{ij}/d_{ik}\right)^{\left(\frac{2}{m}-1\right)} \quad (13)$$

$$v_j = \left(\sum_{j=1}^{n}\left(\mu_{ij}\right)^m x_i\right)/\left(\sum_{i=1}^{n}\left(\mu_{ij}\right)^m\right), \forall_j=1,2,\ldots c \quad (14)$$

Where, *'n'* stands for how many data points there,*' vj'* indicates the j^{th} cluster center, *'m'* refers to the fuzziness index m € [1, ∞], '*c'* signifies how many cluster centres there are, 'μij*'* stands for the membership of i^{th} data to the j^{th} cluster center, '*dij'* refers to the Euclidean distance between i^{th} data and j^{th} cluster center.

The primary aim of the fuzzy c-means is to reduce the:

$$J(u,v)=\sum_{i=1}^{n}\sum_{j=1}^{c}\left(\mu_{ij}\right)^m \left\|x_i - v_j\right\|^2 \quad (15)$$

Where, *' $||x_i - v_j||$'* refers to a distance in Euclidean space between i^{th} data and the j^{th} cluster center.

Algorithmic steps for Fuzzy c-means clustering

Let X = {x_1, x_2, x_3 ..., x_n} refer to the bunch of data points and V = {v_1, v_2, v_3 ..., v_c} indicate the bunch of centres [34-36].

1. choose *'c'* cluster centers in random.
2. Compute the fuzzy membership *'μ_{ij}'* applying (13).
3. Compute the fuzzy centers *' v_j'* applying (14):
4. Repeat steps second and third until the minimum *'J'* value is attained or $||U^{(k+1)} - U^{(k)}|| < \beta$.

4. Results and Discussion

Here, we dissect the experiments that tested the proposed model. To put this concept into action, MATLAB is used. The comparison F-measure, recall, accuracy, and precision are all carried out for the Kaggle brain tumor dataset using the existing ANN and TKMA algorithm and the new FCM.

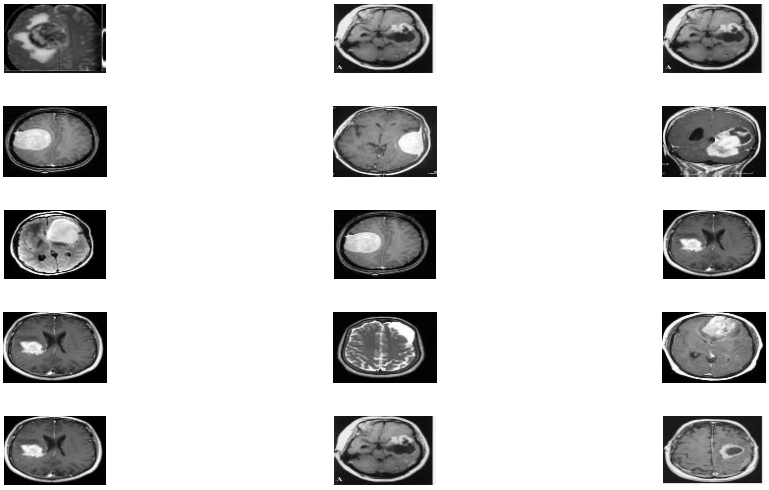

Fig. 2 Input data

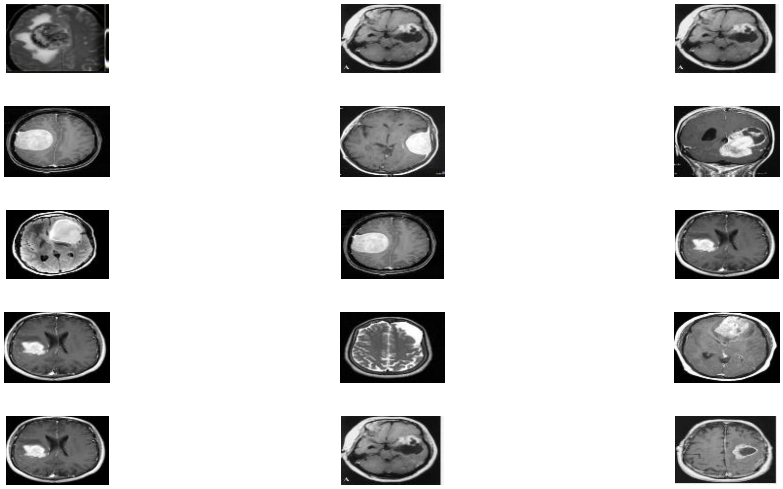

Fig. 3 Noise-removed image

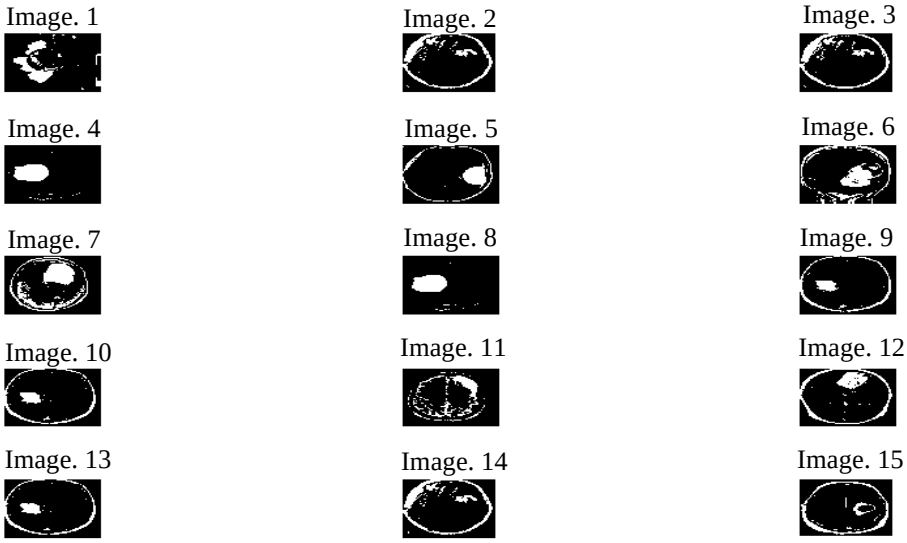

Fig. 4 Segmentation results images

Table 1. Performance comparison results

Metrics	Various Techniques					
	IOGDML	**KMC**	**GEM**	**ANN**	**TKMA**	**FCM**
Accuracy	82.09	83.66	84.23	87.10	91.02	93
Precision	78.03	80.61	82.45	83.01	88	90
Recall	79.02	79.98	83.34	85.23	86.21	97.90
F – measure	78.12	79.45	81.25	84.06	87.10	93.78
Error rate	18.91	16.85	14.77	12.85	10	7

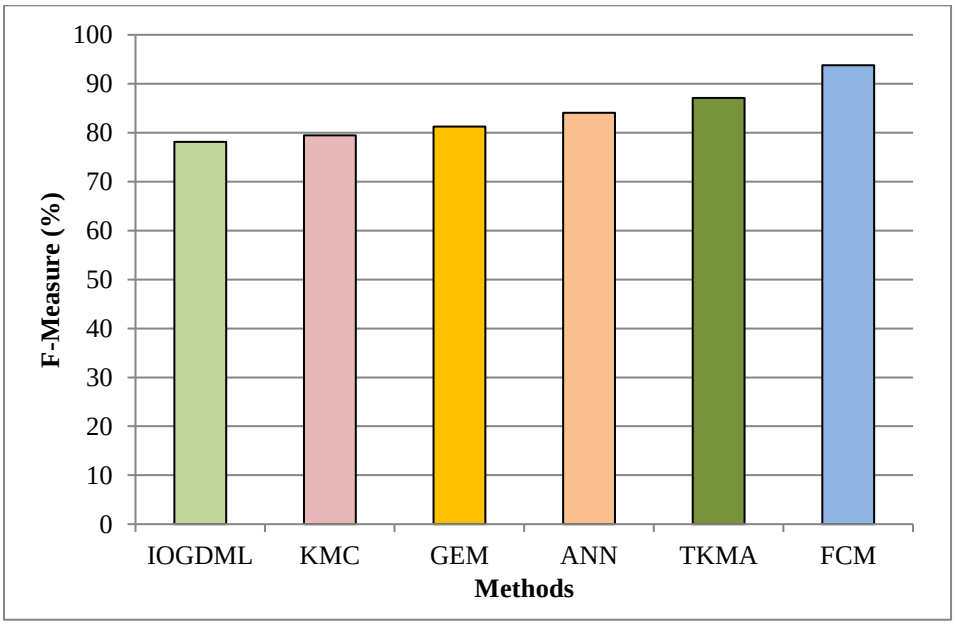

Fig. 5 F- measure results vs Classification methods

Above Figure 2 Shows the input brain images for brain tumor segmentation. Figures 3 and 4 show the pre-processed results images and segmented images. The following graphic displays a performance comparison of the new FCM scheme, the existing IOGDML, KMC, GEM, ANN and TKMA approaches, and the F measure metrics. In the graph mentioned above, the X axis shows the various approaches, while the Y axis depicts the respective F-measure values. The results show that the newly presented FCM model delivered higher F measure outcomes (93.78%) compared to the 78.12%, 79.45%, 81.25%, 84.06% and 87.10% that the available IOGDML, KMC, GEM, ANN and TKMA techniques deliver.

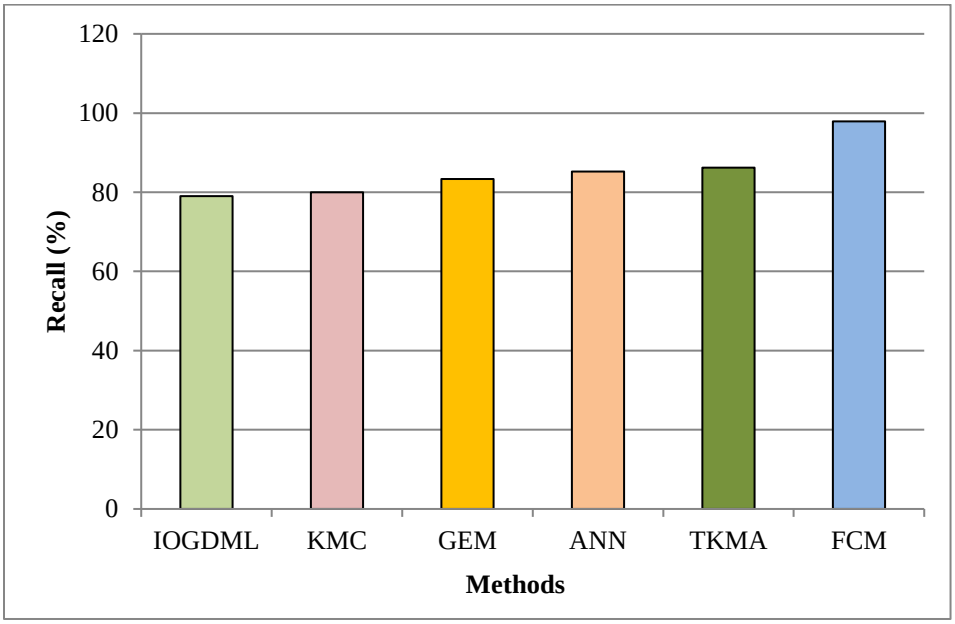

Fig. 6 Recall results vs Classification methods

The above graphic compares the proposed FCM scheme's performance on the Recall metric to that of the existing IOGDML, KMC, GEM, ANN, and TKMA approaches. On the X-axis of the above graph, we see the various approaches, and on the Y-axis, we see the corresponding Recall values. The results show that the newly introduced FCM model achieved a higher Recall of 97.90% compared to the 79.02%,79.98%,83.34%,85.23% and 86.21% achieved by the IOGDML, KMC, GEM, ANN and TKMA techniques, respectively.

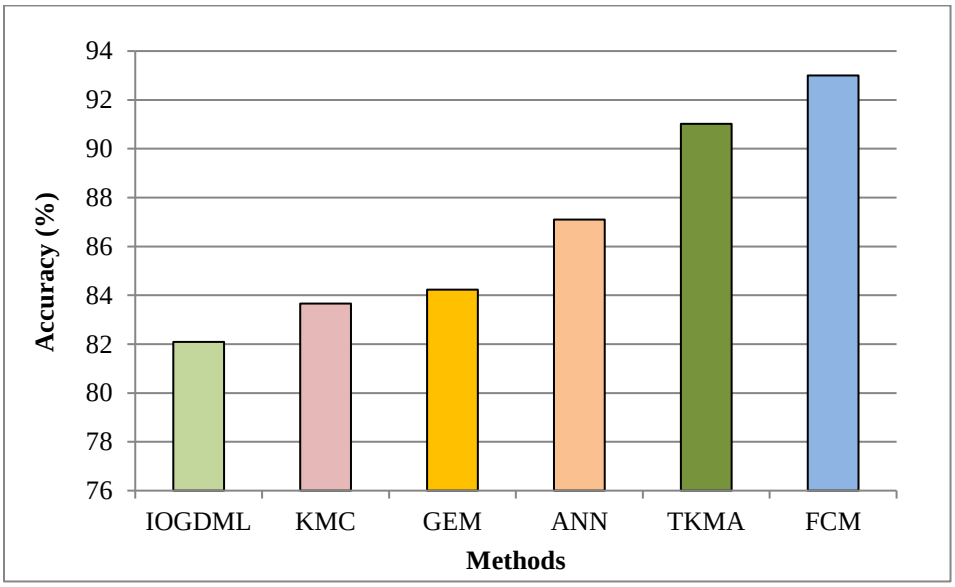

Fig. 7 Accuracy results vs Classification methods

The above diagram contrasts the proposed FCM scheme's accuracy metric performance with the existing IOGDML, KMC, GEM, ANN, and TKMA approaches. The graph above depicts the accuracy of various procedures along the X-axis and the methods along the Y-axis. The results show that the newly presented FCM model achieved greater Accuracy outcomes (93%) compared to the IOGDML, KMC, GEM, ANN and TKMA techniques (which only produce 82.09%,83.66%,84.23%, 87.10% and 91.02%, respectively).

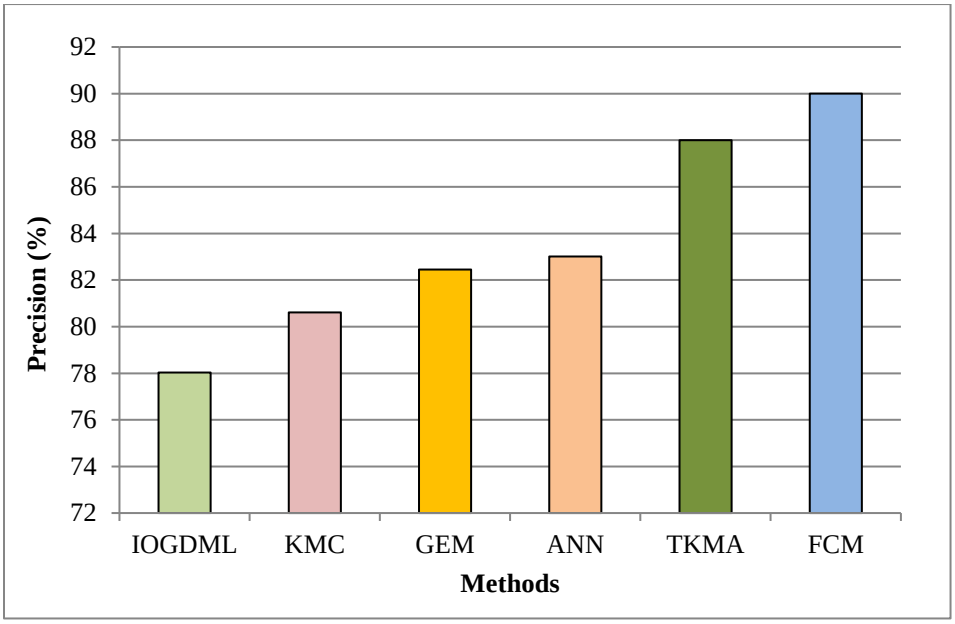

Fig. 8 Precision results vs Classification methods

The above diagram contrasts the new FCM scheme's performance using Precision measures to those of the existing IOGDML, KMC, GEM, ANN, and TKMA approaches. The various techniques are plotted along the X-axis, and the corresponding precision values are shown along the Y-axis. The results show that the newly presented FCM model achieved higher Precision outcomes of 90% compared to the 78.03%, 80.61%,82.45%, 83.01% and 88% that the existing ANN and TKMA approach yields.

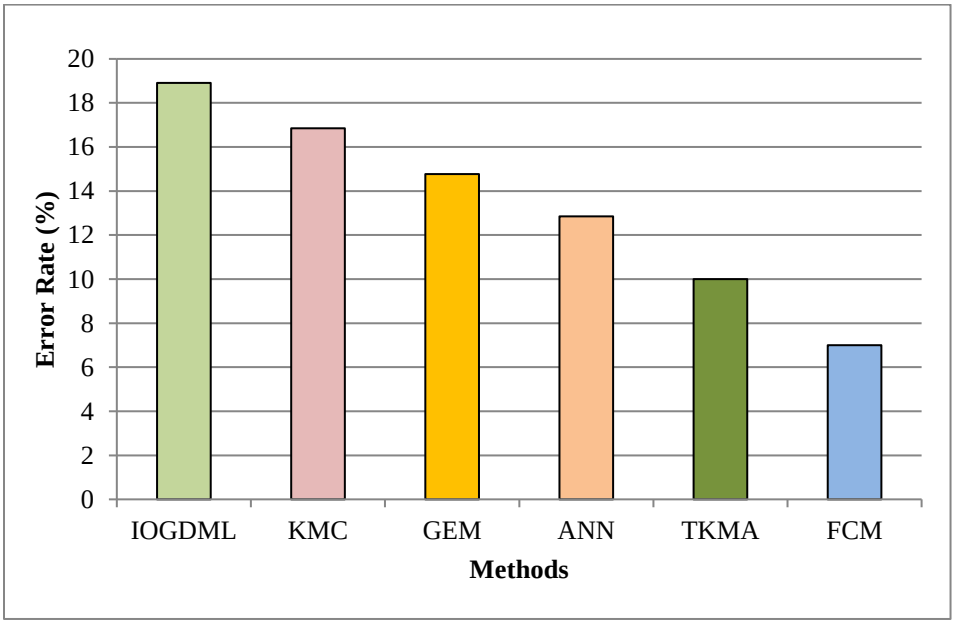

Fig. 9 Error rate results vs Classification methods

The above diagram contrasts the new FCM scheme's performance using Error rate measures to those of the existing IOGDML, KMC, GEM, ANN, and TKMA approaches. The various techniques are schemed along the X-axis, and the corresponding Error rate values are shown along the Y-axis. The results show that the newly presented FCM model achieved higher Error rate outcomes of 7% compared to the 18.91%, 16.85%, 14.77%, 12.85% and 10% that the existing IOGDML, KMC, GEM, ANN and TKMA approach yields.

5. Conclusion and Future Work

Medical image segmentation is both crucial and difficult. It is commonly employed for the diagnosis of cancer. In this study, we focus on how to spot tumors in brain MR scans. Here, we perform some preliminary processing on raw brain MRI data to improve its quality. This processing is centred on converting colour images (RGB) to a grayscale image and eliminating noise with a median filter. Once the images have been improved, the GLCM approach extracts the five statistical texture parameter features. Reduce the file size of an image by using a dimensionality reduction technique like the Independent Component Analysis (ICA) model. Finally, brain tumors are identified, and the segmentation is performed with the help of clustering FCM. Compared to the baseline model, the suggested model significantly improves accuracy. However, FCM results in an apriori specification of the number of clusters. Therefore, we will have to employ different segmentation techniques in the future.

References

[1] Anjali Wadhwa, Anuj Bhardwaj, and Vivek Singh Verma, "A Review on Brain Tumor Segmentation of MRI Images," *Magnetic Resonance Imaging*, vol. 61, pp. 247-259, 2019. [CrossRef] [Google Scholar] [Publisher Link]

[2] Krishna Prajapati et al., "Design and Development of Algorithms for Enhancement of Brain Tumor from Medical Images," *International Journal of Engineering Trends and Technology*, vol. 67, no. 3, pp. 141-145, 2019. [CrossRef] [Publisher Link]

[3] Jin Liu et al., "A Survey of MRI-Based Brain Tumor Segmentation Methods," *Tsinghua Science and Technology*, vol. 19, no. 6, pp. 578-595, 2014. [CrossRef] [Google Scholar] [Publisher Link]

[4] Nooshin Nabizadeh, and Miroslav Kubat, "Brain Tumors Detection and Segmentation in MR Images: Gabor Wavelet vs. Statistical Features," *Computers & Electrical Engineering*, vol. 45, pp. 286-301, 2015. [CrossRef] [Google Scholar] [Publisher Link]

[5] Meiyan Huang et al., "Brain Tumor Segmentation Based on Local Independent Projection-Based Classification," *IEEE Transactions on Biomedical Engineering*, vol. 61, no. 10, pp. 2633-2645, 2014. [CrossRef] [Google Scholar] [Publisher Link]

[6] Mohammad Havaei, Pierre-Marc Jodoin, and Hugo Larochelle, "Efficient Interactive Brain Tumor Segmentation as Within-Brain kNN Classification," *In 2014 22nd International Conference on Pattern Recognition*, pp. 556-561, 2014. [CrossRef] [Google Scholar] [Publisher Link]

[7] Mahmoud Al-Ayyoub et al., "A GPU-Based Implementations of the Fuzzy C-Means Algorithms for Medical Image Segmentation," *The Journal of Supercomputing*, vol. 71, no. 8, pp. 3149-3162, 2015. [CrossRef] [Google Scholar] [Publisher Link]

[8] Aratakatla Hari Kusuma, and P. Mohana Roopa, "An Efficient Clustering Process using Optimized C Means Algorithm in Social Media Data," *International Journal of Computer & Organization Trends (IJCOT)*, vol. 8, no. 2, pp. 34-38, 2018. [Publisher Link]

[9] Gunasekaran Manogaran et al., "Machine Learning Approach-Based Gamma Distribution for Brain Tumor Detection and Data Sample Imbalance Analysis," *IEEE Access*, vol. 7, pp. 12-19, 2018. [CrossRef] [Google Scholar] [Publisher Link]

[10] R. Sakthi Prabha, and M. Vadivel, "Brain Tumor Stages Prediction using FMS-DLNN Classifier and Automatic RPO-RG Segmentation," *SSRG International Journal of Electrical and Electronics Engineering*, vol. 10, no. 2, pp. 110-121, 2023. [CrossRef] [Publisher Link]

[11] G. R. Meghana, Suresh Kumar Rudrahithlu, and K. C. Shilpa, "Detection of Brain Cancer using Machine Learning Techniques A Review," *SSRG International Journal of Computer Science and Engineering*, vol. 9, no. 9, pp. 12-18, 2022. [CrossRef] [Publisher Link]

[12] J. Vijay, and J. Subhashini, "An Efficient Brain Tumor Detection Methodology using K-Means Clustering Algorithm," *In 2013 International Conference on Communication and Signal Processing*, pp. 653-657, 2013. [CrossRef] [Google Scholar] [Publisher Link]

[13] V. Amsaveni, and N. Albert Singh, "Detection of Brain Tumor using Neural Network," *In 2013 Fourth International Conference on Computing, Communications and Networking Technologies (ICCCNT)*, pp. 1-5, 2013. [CrossRef] [Google Scholar] [Publisher Link]

[14] Varsha Nemade, Sunil Pathak, and Ashutosh Kumar Dubey, "Hybrid Deep Convolutional Neural Network Approach for Detecting Breast Cancer in Mammography Images," *SSRG International Journal of Electrical and Electronics Engineering*, vol. 10, no. 5, pp. 102-119, 2023. [CrossRef] [Publisher Link]

[15] Sitanaboina S L Parvathi, and Harikiran Jonnadula, "A Hybrid Semantic Model for MRI Kidney Object Segmentation with Stochastic Features and Edge Detection Techniques," *International Journal of Engineering Trends and Technology*, vol. 70, no. 9, pp. 411-420, 2022. [CrossRef] [Publisher Link]

[16] Ahmad Chaddad, Pascal O Zinn, and Rivka R Colen, "Brain Tumor Identification using Gaussian Mixture Model Features and Decision Trees Classifier," *In 2014 48th Annual Conference on Information Sciences and Systems (CISS)*, pp. 1-4, 2014. [CrossRef] [Google Scholar] [Publisher Link]

[17] Sindhia, Ramanitharan, Shankar Mahalingam, and Soundarya Prithiesh, "Brain Tumor Detection using MRI by Classification and Segmentation," *SSRG International Journal of Medical Science*, vol. 6, no. 3, pp. 12-14, 2019. [CrossRef] [Google Scholar] [Publisher Link]

[18] Rohan K. Gajre, Savita A. Lothe, and Santosh G. Vishwakarma, "Identification of Brain Tumor using Image Processing Technique: Overviews of Methods," *SSRG International Journal of Computer Science and Engineering*, vol. 3, no. 10, pp. 48-52, 2016. [CrossRef] [Google Scholar] [Publisher Link]

[19] Fareed M. Mohammed, Mustafa M. Essa, and Ahmed W. Maseer, "Comparison between MRI and CT-Scan in Diagnosis the Brain Tumor Images," *SSRG International Journal of Medical Science*, vol. 6, no. 5, pp. 1-4, 2019. [CrossRef] [Publisher Link]

[20] Vidyasagar Talwar, and B. S. Sohi, *"*Dimensionality Reduction of Hyperspectral Image using Different Methods*"* *International Journal of Engineering Trends and Technology*, vol. 69, no. 2, pp. 39-143, 2021. [CrossRef] [Publisher Link]

[21] Ibrahima Sory keita et al., "Classification of Benign and Malignant MRIs using SVM Classifier for Brain Tumor Detection," *International Journal of Engineering Trends and Technology*, vol. 70, no. 3, pp. 234-240, 2022. [CrossRef] [Publisher Link]

[22] Ravi Ningappa, and Bagath Singh K, "Study of Brain Mass Lesions by MRI- on Special Sequences," *SSRG International Journal of Medical Science*, vol. 2, no. 2, pp. 1-10, 2015. [CrossRef] [Publisher Link]

[23] T. Gayathri, and K. Sundeep Kumar, "AlexNet - Adaptive Whale Optimisation – Multiclass Support Vector Machine Model for Brain Tumor Classification," *International Journal of Engineering Trends and Technology*, vol. 70, no. 5, pp. 309-316, 2022. [CrossRef] [Publisher Link]

[24] T. Tamilselvi et al., "Deep Derma Scan: A Proactive Diagnosis System for Predicting Malignant Skin Tumor with Deep Learning Mechanisms," *International Journal of Engineering Trends and Technology*, vol. 70, no. 8, pp. 310-317, 2022. [CrossRef] [Publisher Link]

[25] V. Ravindra Krishna Chandar, and M. Thangamani, "Suppression of Noises using Fast Independent Component Analysis and Signal Saturation using Fuzzy Adaptive Histogram Equalization for Intensive Care Unit False Alarms," *Measurement*, vol. 145, pp. 400-409, 2019. [CrossRef] [Google Scholar] [Publisher Link]

[26] S. Suhas, and C. R. Venugopal, "MRI Image Pre-Processing and Noise Removal Technique using Linear and Nonlinear Filters," *In 2017 International Conference on Electrical, Electronics, Communication, Computer, and Optimisation Techniques (ICEECCOT)*, pp. 1-4, 2017. [CrossRef] [Google Scholar] [Publisher Link]

[27] Mellisa Pratiwi et al., "Mammograms Classification using Gray-Level Co-Occurrence Matrix and Radial Basis Function Neural Network," *Procedia Computer Science*, vol. 59, pp. 83-91, 2015. [CrossRef] [Google Scholar] [Publisher Link]

[28] Khin Nyein Nyein Hlaing, and Anilkumar Kothalil Gopalakrishnan, "Myanmar Paper Currency Recognition using GLCM and k-NN," *In 2016 Second Asian Conference on Defence Technology (ACDT)*, pp. 67-72, 2016. [CrossRef] [Google Scholar] [Publisher Link]

[29] Gholamreza Salimi-Khorshidi et al., "Automatic Denoising of Functional MRI Data: Combining Independent Component Analysis and Hierarchical Fusion of Classifiers," *NeuroImage*, vol. 90, pp. 449-468, 2014. [CrossRef] [Google Scholar] [Publisher Link]

[30] Toufique Ahmed Soomro et al., "Impact of ICA-Based Image Enhancement Technique on Retinal Blood Vessels Segmentation," *IEEE Access*, vol. 6, pp. 3524-3538, 2018. [CrossRef] [Google Scholar] [Publisher Link]

[31] Junshi Xia et al., "Spectral–Spatial Classification of Hyperspectral Images using ICA and Edge-Preserving Filter via An Ensemble Strategy," *IEEE Transactions on Geoscience and Remote Sensing*, vol. 54, no. 8, pp. 4971-4982, 2016. [CrossRef] [Google Scholar] [Publisher Link]

[32] Nicola Falco, Jón Atli Benediktsson, and Lorenzo Bruzzone, "Spectral and Spatial Classification of Hyperspectral Images Based on ICA and Reduced Morphological Attribute Profiles," *IEEE Transactions on Geoscience and Remote Sensing*, vol. 53, no. 11, pp. 6223-6240, 2015. [CrossRef] [Google Scholar] [Publisher Link]

[33] Xiangzhi Bai et al., "Intuitionistic Center-Free FCM Clustering for MR Brain Image Segmentation," *IEEE Journal of Biomedical and Health Informatics*, vol. 23, no. 5, pp. 2039-2051, 2019. [CrossRef] [Google Scholar] [Publisher Link]

[34] Souleymane Balla-Arabé, Xinbo Gao, and Bin Wang, "A Fast and Robust Level Set Method for Image Segmentation using Fuzzy Clustering and Lattice Boltzmann Method," *IEEE Transactions on Cybernetics*, vol. 43, no. 3, pp. 910-920, 2013. [CrossRef] [Google Scholar] [Publisher Link]

[35] D. Napoleon, and M. Praneesh, "Detection of Brain Tumor using Kernel Induced Possiblistic C-Means Clustering," *International Journal of Computer Organization Trends and Technology (IJCOT)*, vol. 3, no. 5, pp. 40-42, 2013. [Google Scholar] [Publisher Link]

[36] Lu Xiong et al., "Color Disease Spot Image Segmentation Algorithm Based on Chaotic Particle Swarm Optimisation and FCM," *The Journal of Supercomputing*, vol. 76, no. 11, pp. 8756-8770, 2020. [CrossRef] [Google Scholar] [Publisher Link]